MTLA 28 (2023) 101724

Contents lists available at ScienceDirect

Materialia

journal homepage: www.elsevier.com/locate/mtla

Rapid chemical vapor deposition of graphitic carbon nitride films

Eugene B. Chubenko *, Sergey E. Maximov, Cong Doan Bui, Van Tung Pham, Victor E. Borisenko

Department of Micro- and Nanoelectronics, Belarusian State University of Informatics and Radioelectronics, 6 P. Browka Str., Minsk 220013, Belarus

ARTICLE INFO

Keywords:
Chemical vapor deposition
Thin films
Carbon nitride
Scanning electron microscopy
X-ray diffraction

ABSTRACT

Rapid chemical vapor deposition of continuous thin films of graphitic carbon nitride (g-CN) material with stoichiometry close to its ideal g-C_3N_4 form on silicon and glass substrates is demonstrated. It allows fabrication of 200–1200 nm g-CN films within 3–5 min at 500–620 °C instead of earlier reported few hours. SEM, XRD and EDX analysis of the films revealed their grain-layered structure and high crystallinity. The film thickness and crystallinity were found to have maximum at synthesis temperature of 575–600 °C. Energy band gap of the material changes with the deposition temperature too and reaches its maximum of 2.98 eV at 600 °C. Dependence of the film properties on the deposition temperature evidences competition between the rates of synthesis and evaporation of the synthesized material. The developed approach is energy budget saving and could be scaled up using conventional rapid thermal processing equipment opening a way to practical g-CN based electronics and optoelectronics.

1. Introduction

Chemical vapor deposition (CVD) with separated source and substrate spaces involving gas transport process has been recently demonstrated to be an appropriate technique for fabrication of g-CN films of 10–130 nm [1–5] to about a micrometer [6] thicknesses. As far as material of the films has semiconducting properties ($E_g \sim 2.7$ eV) and high refractive index ($n = 2.43…2.54$) they are considered for optoelectronic and photocatalytic applications [1–6]. Moreover, deposited films were found to have a 2D crystallized layered structure indeed promising for a design of novel nanoelectronic and optoelectronic devices [6,7].

CVD of g-CN films differs from conventional synthesis of this material performed by thermal processing of carbon and nitrogen containing compounds in a closed crucible reactor thus producing only bulk, powder-like products or flakes located at the bottom part of crucible suitable mostly for photocatalytic applications [8–10]. While already fabricated flakes could be incorporated into other materials to obtain continuous coatings [11–14], such coatings have pores and rough surfaces which can not be accepted for fabrication of electronic devices. However, it was demonstrated that g-CN films of high planarity could also be produced on the surface of the substrate placed over the crucible as a cover during the deposition process [15,16]. Described so called thermal vapor condensation (TVC) method could also be considered as "CVD-like" despite the fact that the places of evaporation and condensation is only slightly distanced from each other.

In all cases the earlier proposed CVD of g-CN films [1–7,15,16] typically lasts for hours with rather slow heating (at 5–20 °C/min to 550–600 °C) and slow cooling of the substrates like during conventional bulk synthesis of this material [17–19]. Long heating and cooling cycles mask peculiarities of the film formation. Usually the environment during the deposition is inert nitrogen (N_2) or argon atmosphere or vacuum [1,3,4,16,20]. However, it was found that presence of oxygen during the deposition in ambient atmosphere nether prevent g-CN formation or affect the process. Moreover, the improvement influence on stability and optical properties of the films deposited in air compared to N_2 atmosphere was revealed [21].

Using our previous experience with rapid thermal processing of semiconductors [22] we developed a technique similar to TVC process providing CVD of g-CN films with stoichiometry close to ideal g-C_3N_4 within few minutes with the heating/cooling rates increased up to 5 °C/s. We skipped the heating and cooling stages by placing the substrate and precursor in already heated furnace. The reduced thermal budget of the deposition process gives a possibility of a deeper look at the mechanisms involved in the film formation. The results obtained are presented and discussed in this paper.

2. Methods

Accessories and main steps of the developed rapid CVD of g-CN films are illustrated in Fig. 1.

* Corresponding author.
E-mail address: eugene.chubenko@gmail.com (E.B. Chubenko).

https://doi.org/10.1016/j.mtla.2023.101724
Received 22 November 2022; Accepted 21 February 2023
Available online 24 February 2023

A thin glass funnel with a porous glass membrane inside was used as both precursor material container and substrate holder. The outer diameter of the funnel was 44 mm. The membrane had the thickness of about 4 mm and chaotic throughout pores up to 100 μm in size and was made of fused glass particles. A substrate was placed on the top of the funnel so it was about 30 mm far from the closest membrane surface and precursor material on it. The funnel was mounted into metallic wire support with the lowest possible heat conductance providing its rapid heating and cooling.

Melamine (Sigma-Aldrich) with the purity of 99% was used as a precursor material. Monocrystalline n^+-type silicon (111) and (100) wafers 76 mm in diameter as thick as 380 μm both with 290 nm of silicon oxide (SiO_2) on their surfaces and without it were used as substrates (JSC "Integral", Belarus). Microscope glass slides 25.4 × 76.2 × 1 mm in size with polished edges (ApexLab, China) were also tested as substrates.

The funnel supplied with 150 mg of melamine and a substrate on the top was rapidly put into an air-filled muffle furnace Nabertherm 9 L/330 already stabilized at a certain target temperature in the range of 550–620 °C and kept there for 3–7 min. The substrate was extracted from the furnace first and placed onto the point contact support for cooling down to the room temperature. Then we extracted the funnel. In order to estimate dynamics of heating and cooling processes we recorded time-temperature profiles of the substrate and porous membrane with chromel-alumel thermocouples before the experiments. Their examples for the stabilized furnace temperature of 600 °C are shown in Fig. 1.

The film morphology was analyzed with scanning electron microscopy (SEM) by Hitachi S-4800 SEM. To improve the contrast of the SEM images in some cases thin layers of gold were sputtered on the cross-section of the samples on IB-5 ion beam sputtering system. Bruker QUANTAX 200 energy-dispersive X-ray (EDX) spectrometer was used to study the atomic composition of the films. Crystalline phases in the films were identified by grazing-angle X-ray diffraction analysis (XRD) using DRON-4 diffractometer equipped with Cu *Kα* source (λ = 1.5406 Å). The thickness of the films was calculated from weight measurements of the substrates before and after film deposition with the accuracy of 0.1 mg and compared to the data provided by SEM. Light transmission and reflection of the films at room temperature were determined by Proscan MC121 spectrometer. Photoluminescence (PL) spectra were also recorded at room temperature with SOLAR TII MS7504i spectrophotometer equipped with Proscan HS101 CCD camera as a detector. Narrow monochromatic lines were cut from the broad radiation spectra of the 1000 W xenon lamp by SOLAR TII DM 160 double monochromator to excite PL of the samples. Light with 345 nm wavelength corresponding to 3.59 eV was used for the PL excitation.

3. Results and discussion

Typical cross-section SEM images of the deposited films with high magnification as illustrated in Fig. 2 demonstrate them to have a grain-layered structure with a smooth surface. Each single layer has approximately 30 nm thickness and preferably lies parallel to the surface of the silicon substrate. The thickness of the obtained films measured using SEM images (see Fig. S.1 in Supplementary Materials section) rises with the synthesis temperature from 800 nm at 525 °C up to 1180 nm at 575 °C and then drops to 813 nm with the further temperature growth to 600 °C. Note, that there was no principle difference observed in the structure of the films fabricated on (100), (111) and oxidized silicon substrates.

Mass change of the substrates as a function of the processing temperature for different times demonstrates a nonlinear behavior shown in Fig. 2b. The mass change data were recalculated into the film thicknesses using their surface area and bulk density of g-C_3N_4 which is known to be in the range of 1.9–2.2 g/cm^3 [23]. The best agreement between the calculated thicknesses and direct SEM measurements was achieved for the material bulk density of 1.9 g/cm^3. The lowest in the range bulk density looks reasonable accounting for the grain-layered structure of the films with extended interfaces between the grains.

According to the EDX analysis the films primarily consist of carbon, nitrogen and oxygen (Table 1). More details are presented in Table S.1

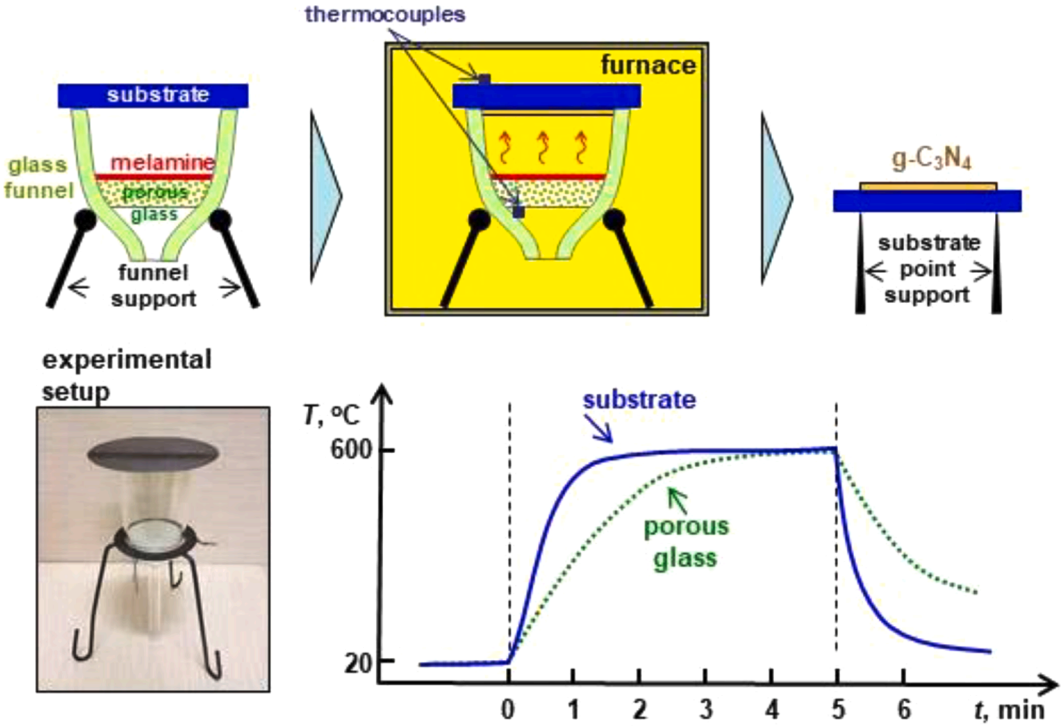

Fig. 1. Rapid chemical vapor deposition of g-CN films from melamine source, the photograph of the experimental setup and time-temperature profiles at the substrate and porous glass membrane holding melamine measured for 600 °C target temperature. First drawing of the deposition scheme indicates the position of thermocouples.

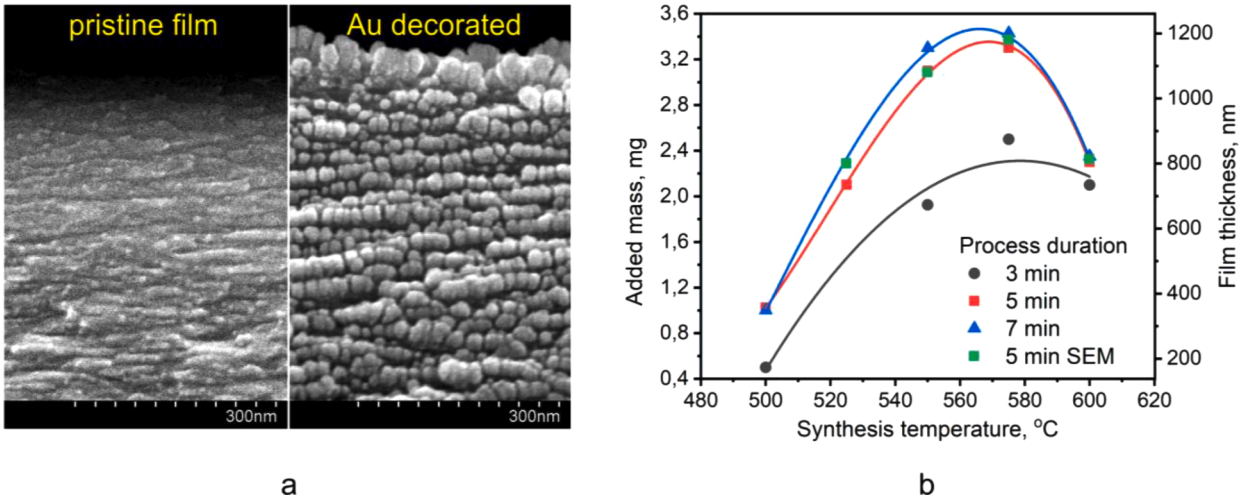

Fig. 2. Cross-section SEM images of the film deposited at 600 °C for 5 min onto silicon (100) substrate (a) and the thickness of the deposited films measured using SEM data labeled as "5 min SEM" and added mass change of the substrates (b). Points on the graphs are connected by polynomial functions.

Table 1
EDX and XRD characteristics of the deposited films.

Deposition temperature, °C	EDX				XRD			
	Element concentration, at.%			C_C/C_N	Peak position, deg	Interplane distance, Å	FWHM, deg	Grain size, nm
	C_C	C_N	C_O					
550	38.2	58.8	2.9	0.650	27.40	3.25	1.35	52.4
575	38.6	58.9	2.5	0.655	27.45	3.25	1.01	69.8
600	38.6	59.0	2.4	0.654	27.46	3.24	1.03	68.4
620	39.4	58.2	2.4	0.677	27.50	3.24	1.00	70.7

and Fig. S.2 in Supplementary Materials section. Oxygen is evident to come from the ambient atmosphere serving as a carrier media during the deposition process. Oxygen content slightly drops from 2.9 to 2.4 at.% with the deposition temperature while carbon/nitrogen atomic ratio increases from 0.65 to 0.677 at the same time.

XRD patterns presented in Fig. 3, a demonstrate single prominent peak at 2θ = 27.4…27.5 deg similar to typical reflection from (002) plane of g-C_3N_4 (polymerized cross-linked melon) phase [24,25] crystallized into hexagonal lattice. Therefore, further we will label the

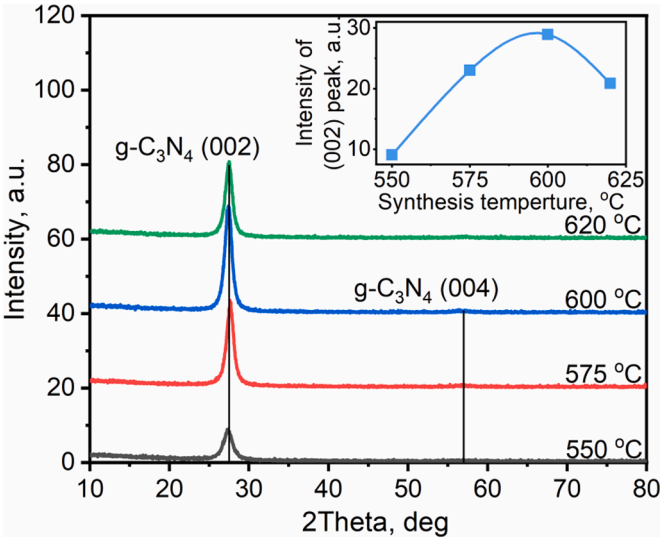

Fig. 3. XRD patterns and intensity of (002) peak (insert) for the g-CN films deposited on silicon at different temperatures during 5 min.

fabricated material as "g-CN" without specifying the exact composition. Despite the vast number of polymorph modifications of carbon nitride [26] revealed C/N ratio and characteristic XRD peak around 27.5 deg constrict the range of possible structural modification to triazine based g-CN and melon.

The intensity of 27.4…27.5 deg line rises in the deposition temperature range of 550 – 600 °C and then drops at 620 °C (Fig. 3, b) thus correlating with the film thickness versus deposition temperature dependencies. The FWHM of that peak decreases from 1.35 deg to 1.00 deg with the growing deposition temperature. The interplane distance (the distance between monolayer sheets of polymerized heptazine units) calculated according to the XRD data also decreases gradually from 3.25 to 3.24 Å with the temperature. It is also should be noted, that despite the small thickness of the deposited films, peaks from silicon substrate are not visible, since XRD patterns were recorded using grazing-angle approach. A weak peak at 2θ = 57 deg is hardly resolved. It corresponds to the reflection from (004) plane of g-C_3N_4 [24].

Fabricated g-CN films demonstrate bright broad band PL in the visible range (Fig. 4a, b) on both silicon and glass substrates. Its peak intensity changes with the film deposition temperature (insert in Fig. 4a). For silicon substrates it undergoes blue shift from 2.62 to 2.65 eV within 550–600 °C range and then moves to 2.62 eV back again when the temperature reaches 620 °C. For glass substrates the PL maximum stays around 2.61 eV within deposition temperature range of 550–575 °C and then shifts to 2.56 eV with the growing temperature. The observed broad band PL spectra are an indication that a few luminescent centers are active in the film material.

Tauc plots (Fig. 4c) calculated using optical transmittance T, reflectance R and film thickness d extracted from SEM images allowed determination the optical band gap of the films obtained on the glass substrates. Absorption coefficient α were calculated according to the equation $\alpha = d^{-1} \times \ln[(1-R)^2/T]$ [27]. Band gap dependence on the film

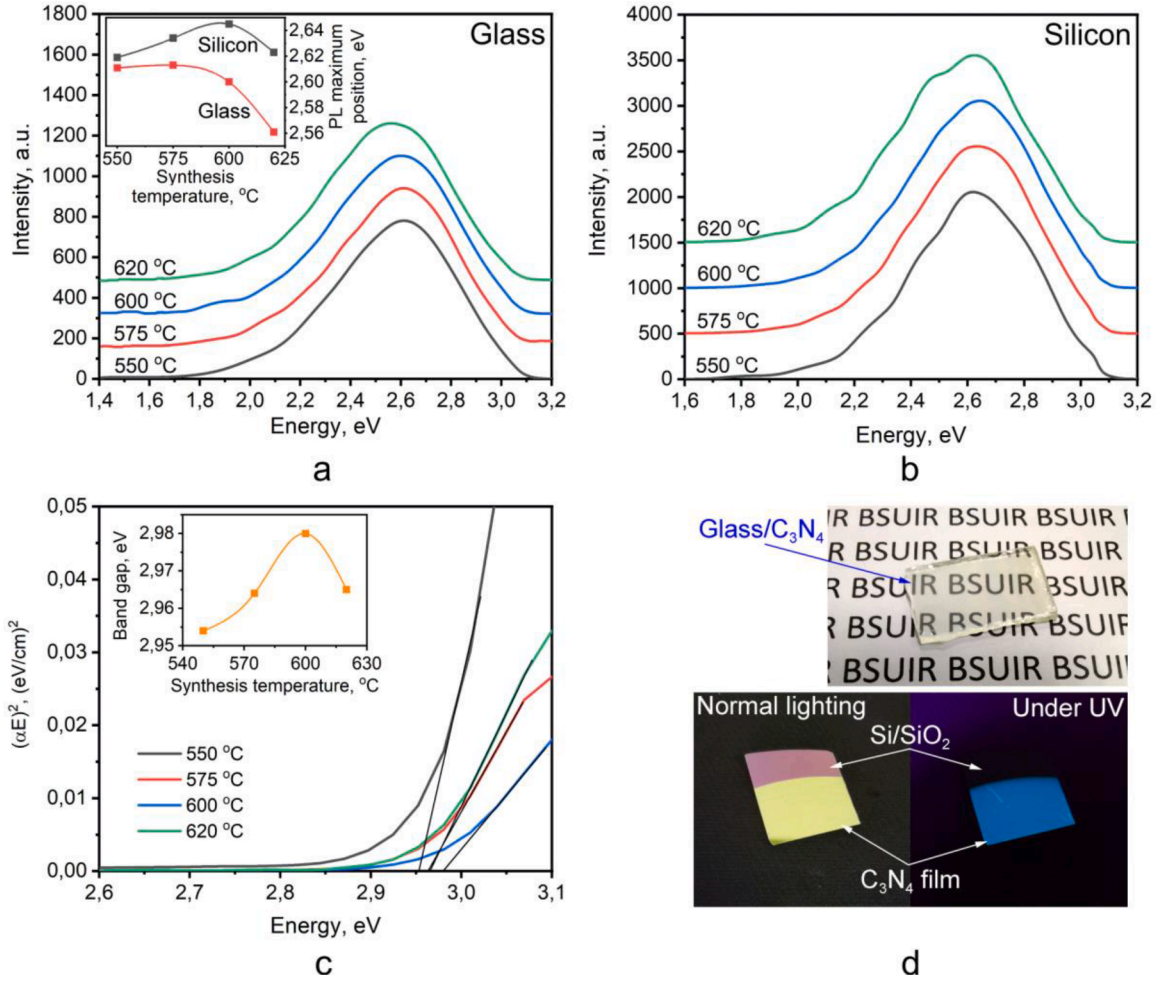

Fig. 4. PL spectra (a, b) and absorption Tauc plots (c) of g-CN films deposited on silicon and glass substrates at different temperatures during 5 min. (d) is the photographs of different substrates covered with g-CN film.

deposition temperature (insert in Fig. 4c) has a concave shape in principle identical to those for the shift of the PL maximum. The extracted optical band gap of 2.95–2.98 eV is about 0.2 eV lager than those registered in bulk undoped g-C_3N_4. It can be an effect of oxygen in our samples.

The photographs of the glass substrate and silicon wafer with SiO_2 sublayer both covered with g-CN film deposited at 600 °C (looks like yellow-gold coating) under normal lighting and UV illumination (monochromatic, 365 nm) are presented on Fig. 4d. The photographs displayed the uniformity, transparency and PL efficiency of the deposited films.

Analyzing the experimental data presented one can note that the atomic ratio C_C/C_N in the deposited material does not reach the stoichiometric one corresponding to 0.75. This is typical for carbon nitride materials not fully polymerized into g-C_3N_4 consisting of melon polymeric chains [25]. Doping by oxygen can also contribute to this difference.

The presence of only interplane g-C_3N_4 (002) peak at the XRD spectra and the absence of g-C_3N_4 (210) peak around $2\theta = 13$ deg charactering in-plane distance between heptazine units in melon chains [24] indicate that the layers of the material are perfectly crystallized with dominant ordering of the hexagonal lattice parallel to the surface of the substrate. The interplane distance between the layers (3.24 – 3.25 Å) is a little bit smaller than 3.26 Å [24] in completely polymerized g-C_3N_4. This compression of the lattice can be a result of slightly nonstoichiometric composition of the material probably enhanced by oxygen dopant.

The observed nonmonotonic dependence of the film thickness and characteristics of the synthesized material on the deposition temperature allows a conclusion that two major competing processes control the film formation by CVD. These are synthesis of g-CN at the substrate surface and evaporation of the already synthesized material. They have temperature dependent rates changing their interplay in the studied processing temperature and time ranges as follows. Synthesis of g-CN on a substrate is supposed to start at about 450 °C as it was observed for the bulk material [8,25]. By the time providing heating of the substrate to this temperature, the melamine holder becomes heated above 340 °C giving rise evaporation of melamine. The evaporated melamine undergoes the chain of chemical transformations to melem, melam and finally to melon [8,24] at higher temperatures. These reactions can take place in the vapor phase close to the heated substrate or more probably directly on its surface. Any case melon is thermally polymerized at the substrate surface producing g-CN sheets as it is confirmed by the experimental fact that hexagonally crystallized layers of the material are arranged with (002) plane parallel to the substrate surface. The observed dependence of the film thickness on the processing time (Fig. 2b) shows that in the temperature range of 500–600 °C synthesis of the film material slows down after the first 5 min. It is an indication that concentration of the precursor at the substrate surface comes to the saturation limiting further increase of the polymerization rate of melon molecules into sheets of g-CN.

Evaporation of the already synthesized g-CN is known to proceed in parallel with its synthesis [8,25]. A competition between these processes becomes indeed evident in the rapid CVD performed. The increase of the film thickness in the deposition temperature range from 500 °C to 575 °C

shows synthesis to proceed faster than evaporation. At higher temperatures the evaporation starts playing a role thus reducing the thickness of the fabricated film. Note here that our attempt to fabricate g-CN film by rapid CVD at 650 °C had no success. There was no deposited material detected on silicon substrates.

The C_C/C_N ratio in the films constantly increases throughout the studied deposition temperature range which is in contrast to g-CN powders [6,8,18]. It means that during rapid CVD decomposition of g-CN which is responsible for the mass loss in the case of powders plays a minor role. It is also confirmed by the XRD data. The g-C_3N_4 (002) peak became narrower with an increase of the deposition temperature. That fact points on better crystallinity of the material synthesized at higher temperatures.

The evolution of the PL maximum position and optical band gap reflect the changes of material energy bands structure with the synthesis temperature. The widening of band gap in 550–600 °C temperature range can reflect the growing polymerization rate of the material. Observed band gap narrowing at high temperatures is supposed to be a result of building up of π-bond conjugated system based on sp^2-hybrydization [28,29].

4. Conclusions

In conclusion, rapid thermal processing of slice-like substrates (silicon and glass) in the vicinity to melamine powder source was demonstrated for the first time to be suitable for chemical vapor deposition of g-CN films within few minutes using their heating at a rate of about 5 °C/s to 500–620 °C. It is almost two orders faster than by previously reported CVD techniques. Meanwhile, the deposited material has crystalline, highly ordered layered structure with the total thickness of the films up to 1.2 μm which can be varied by a suitable choice of the processing temperature and time. The layers lie parallel to the substrate surface. They are oriented along (002) crystal axis. The deposition temperature has a great impact on the structural and optical properties of the films. The proposed rapid thermal processing approach allowed clear observation of the competition between synthesis and evaporation of g-CN. Thus, annealing of the already formed films can be used to make them thinner.

We believe that conventional rapid thermal processing apparatus, in particular with both side substrate heating, can be adopted to realize the regimes demonstrated in this letter to scale up the g-CN deposition procedure. The demonstrated approach opens possibilities to adopt g-CN to optoelectronics and nanoelectronics.

Declaration of Competing Interest

The authors declare that they have no known competing financial interests or personal relationships that could have appeared to influence the work reported in this paper.

Acknowledgments

The authors are grateful to D.V. Zhigulin for the SEM and EDX analysis. The authors declare no conflicts of interests. This work was funded by the Ministry of Education of the Republic of Belarus, Project 1.4, Belarus State Research Program “Material science, novel materials and technologies”; Belarusian Republican Foundation for Fundamental Research, Grant F22–114.

Supplementary materials

Supplementary material associated with this article can be found, in the online version, at doi:10.1016/j.mtla.2023.101724.

References

[1] L. Chen, R. Yan, M. Oschatz, L. Jiang, M. Antonietti, K. Xiao, Ultrathin 2D graphitic carbon nitride on metal films: underpotential sodium deposition in adlayers for sodium-ion batteries, Angew. Chem. Int. Ed. 59 (2020) 9067–9073, https://doi.org/10.1002/anie.202000314.
[2] P.C. Patra, Y.N. Mohapatra, Dielectric constant of thin film graphitic carbon nitride (g-C3N4) and double dielectric Al2O3/g-C3N4, Appl. Phys. Lett. 118 (2021), 103501, https://doi.org/10.1063/5.0045911.
[3] P. Giusto, D. Cruz, T. Heil, H. Arazoe, P. Lova, T. Aida, D. Comoretto, M. Patrini, M. Antonietti, Shine bright like a diamond: new light on an old polymeric semiconductor, Adv. Mater. (2020), 1908140, https://doi.org/10.1002/adma.201908140, 2020.
[4] P. Giusto, B. Kumru, D. Cruz, M. Antonietti, Optical Anisotropy of carbon nitride thin films and photographed polystyrene brushes, Adv. Opt. Mater. 10 (2022), 2101965, https://doi.org/10.1002/adom.202101965.
[5] P. Giusto, H. Arazoe, D. Cruz, P. Lova, T. Heil, T. Aida, M. Antonietti, Boron carbon nitride thin films: from disordered to ordered conjugated ternary materials, J. Am. Chem. Soc. 142 (2020) 20883–20891, https://doi.org/10.1021/jacs.0c10945.
[6] E.B. Chubenko, N.G. Kovalchuk, I.V. Komissarov, V.E. Borisenko, Chemical vapor deposition of 2D crystallized g-C3N4 layered films, J. Phys. Chem. C 126 (2022) 4710–4714, https://doi.org/10.1021/acs.jpcc.1c10561.
[7] H. Arazoe, D. Miyajima, K. Akaike, F. Araoka, E. Sato, T. Hikima, M. Kawamoto, T. Aida, An autonomous actuator driven by fluctuations in ambient humidity, Nat. Mater. 15 (2016) 1084–1090, https://doi.org/10.1038/nmat4693.
[8] A. Thomas, A. Fischer, F. Goettmann, M. Antonietti, J.-O. Müller, R. Schlögl, J. M. Carlsson, Graphitic carbon nitride materials: variation of structure and morphology and their use as metal-free catalysts, J. Mater. Chem. 18 (2008) 4893–4908, https://doi.org/10.1039/B800274F.
[9] J. Zhu, P. Xiao, H. Li, S.A.C. Carabineiro, Graphitic carbon nitride: synthesis, properties, and applications in catalysis, ACS Appl. Mater. Interfaces 6 (2014) 16449–16465, https://doi.org/10.1021/am502925j.
[10] A. Wang, C. Wang, L. Fu, W. Wong-Ng, Y. Lan, Recent advances of graphitic carbon nitride-based structures and applications in catalyst, sensing, imaging, and LEDs, Nano Micro Lett. 9 (2017) 47, https://doi.org/10.1007/s40820-017-0148-2.
[11] F. Yang, M. Lublow, S. Orthmann, C. Merschjann, T. Tyborski, M. Rusu, S. Kubala, A. Thomas, R. Arrigo, M. Hävecker, T. Schedel-Niedrig, Metal-free photocatalytic graphitic carbon nitride on p-type chalcopyrite as a composite photocathode for light-induced hydrogen evolution, ChemSusChem 5 (2012) 1227–1232, https://doi.org/10.1002/cssc.201100691.
[12] T. Suter, V. Brazdova, K. McColl, T.S. Miller, H. Nagashima, E. Salvadori, A. Sella, C.A. Howard, C.W.M. Kay, F. Cora, P.F. McMillan, Synthesis, structure and electronic properties of graphitic carbon nitride film, J. Phys. Chem. C 122 (2012) 25183–25194, https://doi.org/10.1021/acs.jpcc.8b07972.
[13] M.N. Uddin, O.A. Fouad, M. Yamazato, M. Nagano, Deposition and characterization of carbon nitride films from hexamethylenetetramine/N2 by microwave plasma-enhanced chemical vapor deposition, Appl. Surf. Sci. 240 (2005) 120–130, https://doi.org/10.1016/j.apsusc.2004.06.020.
[14] J. Safaei, N.A. Mohamed, M.F.M. Noh, M.F. Soh, M.A. Riza, N.S.M. Mustakim, N. A. Ludin, M.A. Ibrahim, W.N.R.W. Isahak, M.A.M. Teridi, Graphitic carbon nitride (g-C3N4) electrodes for energy conversion and storage: a review on photoelectrochemical water splitting, solar cells and supercapacitors, J. Mater. Chem. A. 6 (2018) 22346–22380, https://doi.org/10.1039/C8TA08001A.
[15] J. Bian, Q. Li, C. Huang, J. Li, Y. Guo, M. Zaw, R.-Q. Zhang, Thermal vapor condensation of uniform graphitic carbon nitride films with remarkable photocurrent density for photoelectrochemical applications, Nano Energy 15 (2015) 353–361, https://doi.org/10.1016/j.nanoen.2015.04.012.
[16] C. Jia, L. Yang, Y. Zhang, X. Zhang, K. Xiao, J. Xu, J. Liu, Graphitic carbon nitride films: emerging paradigm for versatile applications, ACS Appl. Mater. Interfaces 12 (2020) 53571–53591, https://doi.org/10.1021/acsami.0c15159.
[17] A. Sudhaik, P. Raizada, P. Shandilya, D.-Y. Jeong, J.-H. Lim, P. Singh, Review on fabrication of graphitic carbon nitride based efficient nanocomposites for photodegradation of aqueous phase organic pollutants, J. Ind. Eng. Chem. 67 (2018) 28–51, https://doi.org/10.1016/j.jiec.2018.07.007.
[18] E.B. Chubenko, N.M. Denisov, A.V. Baglov, V.P. Bondarenko, V.V. Uglov, V. E. Borisenko, Recovery behavior of the luminescence peak from graphitic carbon nitride as a function of the synthesis temperature, Cryst. Res. Technol. 55 (2020), 1900163, https://doi.org/10.1002/crat.201900163.
[19] Y. Wang, L. Liu, T. Ma, Y. Zhang, H. Huang, 2D graphitic carbon nitride for energy conversion and storage, Adv. Funct. Mater. 31 (2021), 2102540, https://doi.org/10.1002/adfm.202102540.
[20] N. Urakami, M. Kosaka, Y. Hashimoto, Thermal chemical vapor deposition and luminescence property of graphitic carbon nitride film for carbon-based semiconductor systems, Jap. J. Appl. Phys. 58 (2019), 010907, https://doi.org/10.7567/1347-4065/aaf225.
[21] P. Prausa, A. Smýkalová, K. Fonioka, V. Matějka, M. Kormunda, B. Smetana, D. Cvejn, The presence and effect of oxygen in graphitic carbon nitride synthetized in air and nitrogen atmosphere, Appl. Surf. Sci. 529 (2020), 147086, https://doi.org/10.1016/j.apsusc.2020.147086.
[22] V.E. Borisenko, P.J. Hesketh, Rapid Thermal Processing of Semiconductors, Plenum, New York, 1997.
[23] E. Kroke, M. Schwarz, Novel group 14 nitrides, Coord, Chem. Rev. 248 (2004) 493–532, https://doi.org/10.1016/j.ccr.2004.02.001.
[24] F. Fina, S.K. Callear, G.M. Carins, J.T.S. Irvine, Structural investigation of graphitic carbon nitride via XRD and neutron diffraction, Chem. Mater. 27 (2015) 2612–2618, https://doi.org/10.1021/acs.chemmater.5b00411.

[25] F.K. Kessler, Y. Zheng, D. Schwarz, C. Merschjann, W. Schnick, X. Wang, M. J. Bojdys, Functional carbon nitride materials – design strategies for electrochemical devices, Materials 2 (2017) 17030, https://doi.org/10.1038/natrevmats.2017.30. Basel.

[26] D. Vidyasagar, T. Bhoyar, G. Singh, A. Vinu, Recent progress in polymorphs of carbon nitride: synthesis, properties, and their applications, Macromol. Rapid Commun. 42 (2021), 2000676, https://doi.org/10.1002/marc.202000676.

[27] D.C. Look, On the accurate determination of absorption coefficient from reflectanceand transmittance measurements: application to Fe-doped GaN, J. Vac. Sci. Technol 34 (2016) 04J105, https://doi.org/10.1116/1.4954211. B.

[28] B. Choudhury, K.K. Paul, D. Sanyal, A. Hazarika, P.K. Giri, Evolution of nitrogen-related defects in graphitic carbon nitride nanosheets probed by positron annihilation and photoluminescence spectroscopy, J. Phys. Chem. C 122 (2018) 9209–9219, https://doi.org/10.1021/acs.jpcc.8b01388.

[29] Y. Jiang, Z. Sun, C. Tang, Y. Zhou, L. Zeng, Enhancement of photocatalytic hydrogen evolution activity of porous oxygen doped g-C3N4 with nitrogen defects induced by changing electron transition, Appl. Catal. B 240 (2019) 30–38, https://doi.org/10.1016/j.apcatb.2018.08.059.